Structural Study of Sodium-Type Zeolite LTA by Combination of Rietveld and Maximum-Entropy Methods

T. Ikeda,*,† F. Izumi,‡ T. Kodaira,§,|| and T. Kamiyama⊥

Institute of Applied Physics, University of Tsukuba, Tsukuba, Ibaraki 305-8573, Japan, National Institute for Research in Inorganic Materials, Tsukuba, Ibaraki 305-0044, Japan, National Institute of Materials and Chemical Research, Tsukuba, Ibaraki 305-8565, Japan, National Institute for Advanced Interdisciplinary Research, Tsukuba, Ibaraki 305-8562, Japan, and Institute of Materials Science, University of Tsukuba, Tsukuba, Ibaraki 305-8573, Japan

Received June 22, 1998. Revised Manuscript Received September 11, 1998

The electron-density distribution in hydrated and dehydrated sodium-type zeolite LTA was visualized from X-ray powder diffraction data by combining Rietveld analysis and a maximum-entropy method. The X-ray diffraction data were analyzed on the basis of the composition $Na_{95}Si_{97}Al_{95}O_{384}$ and a structural model (space group $Fm\bar{3}c$) obtained by the Rietveld refinement of time-of-flight neutron powder diffraction data for the dehydrated sample. Weighted R factors, wR_F, resulting from the analysis by the maximum-entropy method reached 1.15% for the hydrated sample and 0.99% for the dehydrated one. The number of water molecules per unit cell in the hydrated sample was estimated to be ca. 255 by electron-density analysis, agreeing well with ca. 248 determined by thermogravimetry. Adsorbed water molecules are situated beside Na^+ ions in electron-density maps. In contrast with the dehydrated sample, Na^+ ions in eight-membered rings were moved a little by introducing water into the α-cages.

Introduction

The sodium-type zeolite LTA is one of many well-known and popular zeolites with a relatively simple structure (cubic, space group $Fm\bar{3}c$). Structural studies of LTA using high-resolution powder diffraction data mainly dealt with cation distribution and framework topology.[1−6] On the other hand, the locations of water molecules incorporated in its cages are of great interest from a structural point of view. Crystal data of hydrated zeolites provide us with significant information regarding the adsorption behavior of water. As yet little is known of detailed structures for hydrated zeolites[5,6] because of difficulty in locating water in fairly complicated structures including many atoms in their asymmetric units. Several investigations have dealt with crystal structures of zeolites incorporating unstable guest materials.[7,8] Part of structural models adopted in these studies are inconsistent with other experimental facts, which indicates that these models are far from perfect.

Compared with single-crystal diffraction, powder diffraction generally affords us poorer structural information owing to the overlap of reflections. Solving unknown structures is neither easy nor straightforward with powder diffraction data, whose analysis is, however, indispensable when only polycrystalline samples are available. Once initial structural models are constructed by some means, Rietveld refinements with high-resolution powder diffraction data can offer reliable crystal data.

With conventional X-ray powder diffractometers used in routine measurements, high-quality X-ray diffraction (XRD) data are difficult to collect, mainly because of relatively low resolution and marked profile asymmetry in reflections with larger lattice-plane spacings, d. The intensities of such reflections, which lie in a region $2\theta < 20°$ with Cu Kα radiation, are most important to determine occupation factors and disordered arrangements of guests in zeolites. Nevertheless, XRD data have often been analyzed by excluding such large d regions. Detailed information about arrangements and orientations of molecules or clusters in cages or channels cannot be extracted without large d reflections that contribute considerably to electron densities spread off

* Corresponding author.
† Institute of Applied Physics, University of Tsukuba.
‡ National Institute for Research in Inorganic Materials.
§ National Institute of Materials and Chemical Research.
|| National Institute for Advanced Interdisciplinary Research.
⊥ Institute of Materials Science, University of Tsukuba.

(1) Cheetham, A. K.; Eddy, M. M.; Jefferson, D. A.; Thomas, J. M. *Nature* **1982**, *299*, 24.
(2) Adams, J. M.; Haselden, D. A.; Hewat, A. W. *J. Solid State Chem*. **1982**, *44*, 245.
(3) Adams, J. M.; Haselden, D. A. *J. Solid State Chem*. **1983**, *47*, 123.
(4) Adams, J. M.; Haselden, D. A. *J. Solid State Chem*. **1984**, *51*, 83.
(5) Leung, P. C. W.; Kunz, L. B.; Seff, L.; Maxwell, I. E. *J. Phys. Chem*. **1975**, *79*, 2157.
(6) Gramlich, V.; Meier, W. M. *Z. Kristallogr*. **1971**, *133*, 134.
(7) Armstrong, A. R.; Anderson, P. A.; Edwards, P. P. *J. Solid State Chem*. **1994**, *111*, 179.
(8) McCusker, L. B.; Baerlocher, Ch.; Bülow, J. E. M. *Zeolite* **1991**, *11*, 308.

10.1021/cm980442y CCC: $15.00
Published on Web 11/04/1998

atomic nuclei. In the analysis of electron-density distribution (EDD), XRD data in a large *d* region are also essential for clarifying the nature of bonds and poorly defined arrangements of guests.

In this study, we applied (a) an X-ray powder diffractometer equipped with long Soller slits and (b) a Rietveld-analysis program, RIETAN-98, to structure refinements of hydrated and dehydrated Na-LTA. The use of these techniques enables us to fit profiles of large *d* reflections satisfactorily. XRD data of Na-LTA measured on this diffractometer were analyzed by combining Rietveld refinement and a maximum-entropy method (MEM).[9,10] This combinational technique, which has been first applied to zeolites, is expected to afford very distinct EDD maps of both types of Na-LTA. Takata et al.[10] applied a similar procedure to the modeling of structures for metallofullerenes, proving its validity and capacity. Another technique, i.e., the combination of the Le Bail method and the MEM, was also utilized to determine cation distribution in Na-LTA[11] and to model a structure for a similar sodalite compound.[12]

The MEM, which is a versatile approach to estimating information near to the true one,[13] has recently been applied actively to precise determination of EDD.[11,14−17] Imaging EDD by the MEM makes it possible to locate uncertain and/or disordered sites.[10] The MEM infers EDD in such a way that EDD have the maximum variance for observed structure factors within their error ranges. In the absence of small *d* reflections, we can hardly plot reliable Fourier-synthesis maps because of a so-called termination effect. On the contrary, even if we can measure only intensity data where small *d* reflections are lacking, the MEM is capable of estimating nonzero structure factors for unobserved reflections.

Time-of-flight (TOF) neutron powder diffraction was auxiliarily used to determine the exact structure of a framework and the amount of Na^+ ions in the dehydrated sample. Needless to say, neutron and X-ray diffraction are supplementary to each other. In neutron diffraction, the coherent scattering length is constant regardless of *d*, and absorption is nearly negligible in zeolites composed of Al, Si, and O. Furthermore, we can extend the *d* range down to ca. 0.5 Å in TOF neutron powder diffraction, which makes it possible to obtain accurate fractional coordinates and atomic displacement parameters.

Experimental Section

Na-LTA was hydrothermally synthesized from sodium metasilicate nonahydrate, $Na_2SiO_3 \cdot 9H_2O$, and sodium aluminate, $NaAlO_2$, at 97 °C in an open system.[18] Scanning electron microscopy revealed the average size of crystallites to be about 3 μm. The product was washed up to a pH value of ca. 7 to remove excessive Na^+ and OH^- ions. The weight change of this sample on heating to 700 °C was measured by thermogravimetry. The amount of adsorbed water was ca. 248 molecules per unit cell. Hydrated Na-LTA charged in a Pyrex glass tube was dehydrated by heating at 350 °C below 10^{-5} Torr for 72 h. The sample was then cooled to room temperature in 12 h under vacuum to prevent rehydration. Na-LTA dehydrated in this way was finally sealed in a glass tube to be transferred to a glovebox, where partial pressures of O_2 and H_2O in a purified He gas were kept at less than 1 ppm. As described later, the dehydrated sample still contained a slight amount of water in its cages. The ω-scan method[19] showed that both samples scarcely contained coarse crystallites.

The TOF neutron powder diffraction data were taken at room temperature on the Vega diffractometer at the KENS pulsed neutron source. Its instrumental resolution was $\Delta d/d \approx 2 \times 10^{-3}$ with a backward detector bank. The dehydrated sample (7 g) was loaded in a cylindrical vanadium cell with an inner diameter of 10 mm in the glovebox. The cell was rotated during the measurement to suppress a preferred-orientation effect.

The XRD data were collected at room temperature with the Bragg−Brentano-type powder diffractometer (MAC Science MXP 3TZ) with a vertical $\theta-\theta$ configuration. To suppress axial divergence, the goniometer of this diffractometer was equipped with a pair of the long horizontal Soller slits, whose lengths were 52 and 106 mm for incident and diffracted X-rays, respectively. These slits were designed to decrease the angular aperture to 1° and noise arising from fluorescent X-rays. A diffracted-beam monochromator of curved graphite was placed between a receiving slit and a scintillation detector. After the dehydrated sample in the glass tube had been transferred to the glovebox, it was charged in a detachable sample holder of a flat-plate type. The sample holder was then attached to the goniometer for measurements under vacuum ($p < 10^{-5}$ Torr). All the XRD data were measured under the following experimental conditions: radiation, Cu Kα; output, 50 kV and 44 mA; scan range, $5° < 2\theta < 100°$; step width, 0.016°; counting time per step, 60 s for $5° < 2\theta < 38.5°$ and 120 s for $38.5° < 2\theta < 100°$.

Structure Refinement with the Neutron Diffraction Data

The neutron diffraction data of the dehydrated sample in a range 0.80 Å $< d <$ 4.47 Å were analyzed by the Rietveld-refinement program RIETAN-98T optimized for Vega.[20,21] Peak-to-background ratios in the neutron diffraction data were fairly low. This fact is ascribed to (a) relatively small diffraction amplitudes arising from a large unit-cell volume of Na-LTA and (b) profiles being somewhat broadened owing to a lowering of crystallinity caused by the heating at 350 °C. The structural model for our refinement was based on that of Adams et al.[2,3] (space group $Fm\bar{3}c$, No. 226), where Si and Al atoms are completely ordered. Cheetham et al.[1] presented experimental evidence for ordering of Si and Al which obeyed Loewenstine's rule. Nevertheless, XRD data have been usually analyzed without considering such ordering because the atomic scattering factors of Si and Al are comparable to each other. In this model, the amount of substance for Na^+ ions was set equal to that for Al atoms to maintain electrical neutrality. Four oxygen sites, O4, O5, O6, and O7, were added, in accord with the results of X-ray structure

(9) Sakata, M.; Sato, M. *Acta Crystallogr.* **1990**, *A46*, 263.
(10) Takata, M.; Umeda, B.; Nishibori, E.; Sakata, M.; Saito, Y.; Ohno, M.; Shinohara, H. *Nature* **1995**, *46*, 377.
(11) Papoular, R. J.; Cox, D. E. *Europhys. Lett.* **1995**, *32*, 337.
(12) Knorr, K.; Madler, F.; Papoular, R. J. *Microporous Mesoporous Mater.* **1998**, *21*, 353.
(13) Shannon, C. E. *Bell Syst. Technol. J.* **1948**, *27*, 379.
(14) Takata, M.; Sakata, M. *Acta Crystallogr.* **1996**, *A52*, 287.
(15) Iversen, B. B.; Jensen, J. L.; Danielsen, J. *Acta Crystallogr.* **1997**, *A53*, 376.
(16) Bricogne, G. *Acta Crystallogr.* **1984**, *A40*, 410.
(17) Bricogne, G. *Acta Crystallogr.* **1991**, *A47*, 803.
(18) *Inorganic Synthesis*; Holt, S. L., Jr., Ed.; Wiley: NewYork, 1983; Vol. 22, pp 61−68.
(19) Yukino, K.; Uno, R. *Jpn. J. Appl. Phys.* **1986**, *25*, 661.
(20) Ohta, T.; Izumi, F.; Oikawa, K.; Kamiyama, T. *Physica B* **1997**, *234*, 1093.
(21) Izumi, F. In *The Rietveld Method*; Young, R. A., Ed.; Oxford University Press: Oxford, 1995; Chapter 13.

Table 1. Structure Parameters Determined for Dehydrated Na-LTA by TOF Neutron Powder Diffraction[a]

atom	site	*g*	*n*	*x*	*y*	*z*	*B*/Å^2
Si1	96i	1	96.00	0	0.0944(2)	0.1843(2)	
Si2	96i	0.010(9)	0.96	0	0.1887(4)	0.0891(3)	
Al	96i	0.990	95.40	0	=*y*(Si2)	=*z*(Si2)	
O1	96i	1	96.00	0	0.1151(4)	0.2450(2)	
O2	96i	1	96.00	0	0.1446(2)	0.1465(2)	
O3	192j	1	192.00	0.0552(2)	0.05760(14)	0.17086(9)	
Na2	64g	1	64.00	0.10069(15)	=*x*	=*x*	
Na2	96i	0.242(3)	23.24	0	0.2838(9)	0.3049(11)	
Na3	96h	0.057(8)	5.47	1/4	0.052(2)	=*y*	4.7(3)
O4	192j	0.0041(17)	0.77	0.053(6)	0.045(12)	0.057(18)	3.5(6)
O5	192j	=*g*(O1)	0.77	=*y*(O4)	=*x*(O4)	=*z*(O4)	=*B*(O4)
O6	192j	0.014(2)	2.69	0.023(6)	0.792(8)	0.271(62)	3.5(7)
O7	192j	=*g*(O3)	2.69	=*y*(O6)	=*x*(O6)	=*z*(O6)	=*B*(O6)

atom	U_{11}	U_{22}	U_{33}	U_{12}	U_{13}	U_{23}	B_{eq}/Å^2
Si1	1.8(2)	0.4(2)	0.3(2)	0	0	−0.2(2)	0.67
Si2	=U_{11}(Si1)	=U_{22}(Si1)	=U_{33}(Si1)	0	0	=U_{23}(Si1)	0.67
Al	=U_{11}(Si1)	=U_{22}(Si1)	=U_{33}(Si1)	0	0	=U_{23}(Si1)	0.67
O1	5.7(3)	5.1(4)	0.1(24)	0	0	−1.4(4)	2.88
O2	6.2(3)	0.5(3)	2.1(2)	0	0	1.2(2)	2.30
O3	3.7(3)	1.3(3)	2.8(2)	−0.2(1)	0.7(2)	0.7(2)	2.05
Na1	4.8(2)	=U_{11}	=U_{11}	3.2(2)	=U_{12}	=U_{12}	3.76
Na2	1.5(6)	1.5(6)	15.1(9)	0	0	4.3(9)	4.80

[a] Definitions: *g*, occupation factors; *n*, number of atoms per unit cell; *B*, isotropic atomic displacement parameter; B_{eq}, equivalent isotropic atomic displacement parameters. U_{ij}'s are anisotropic atomic displacement parameters (10^{-2} Å^2) when the displacement factor is represented as $\exp[-2\pi^2 (h^2U_{11} + k^2U_{22} + l^2U_{33} + 2hkU_{12} + 2hlU_{13} + 2klU_{23})/a^2]$.

Table 2. Interatomic Distances, *l*, and Bond Angles, ϕ, Obtained for Dehydrated Na-LTA by TOF Neutron Powder Diffraction[a]

l/Å		ϕ/deg	
Si1−O1	1.572(7)	O1−Si1−O2	108.1(5)
Si1−O2	1.543(8)	O1−Si1−O3	111.4(3)
Si1−O3,O3^{i}	1.659(5)	O1−Si1−O3^{i}	111.4(3)
Al1,Si2−O1^{ii}	1.751(7)	O2−Si1−O3	108.3(3)
Al1,Si2−O2	1.780(6)	O2−Si1−O3^{i}	108.3(3)
Al1,Si2−O3^{iii},O3^{iv}	1.694(4)	O3−Si1−O3^{i}	109.2(3)
Na1−O2,O2^{iii},O2^{v}	2.9205(14)	O1^{ii}−Al1,Si2−O2	105.8(3)
Na1−O3,O3^{iii},O3^{v}	2.309(2)	O1^{ii}−Al1,Si2−O3^{iii}	114.77(11)
Na2−O1^{vi}	2.77(3)	O1^{ii}−Al1,Si2−O3^{iv}	114.77(11)
Na2−O1^{vii}	2.18(3)	O2−Al1,Si2−O3^{iii}	103.40(10)
Na2−O2^{vi}	2.12(2)	O2−Al1,Si2−O3^{iv}	103.40(10)
Na2−O2^{vii}	3.59(3)	O3^{iii}−Al1,Si2−O3^{iv}	113.01(12)
Na3−O1^{v}	2.009(10)	Si1−O1−Al1^{vii}	139.6(6)
Na3−O3^{v}	1.948(7)	Si1−O2−Al1	164.3(3)
		Si1−O3−Al1^{v}	143.1(3)

[a] Symmetry codes: (i) $-x, y, z$; (ii) $x, {}^1/_2 - z, y$; (iii) y, z, x; (iv) $-y, z, x$; (v) z, x, y; (vi) $-x, {}^1/_2 - y, {}^1/_2 - z$; (vii) $x, z, {}^1/_2 - y$.

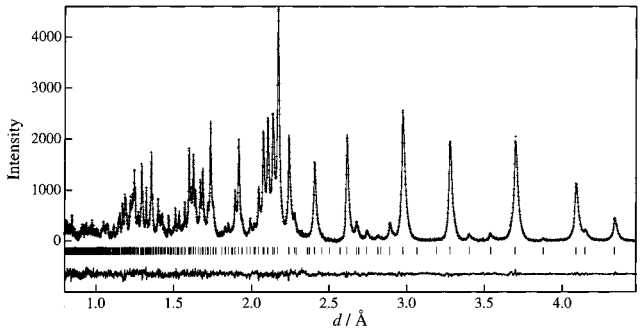

Figure 1. Rietveld-refinement patterns for the TOF neutron powder diffraction data of the dehydrated sodium-type zeolite LTA at room temperature. Observed diffraction intensities are represented by plus (+) marks and the calculated pattern by the solid line. Differences between the observed and calculated intensities are given near the bottom. Short vertical marks below the observed and calculated patterns indicate the positions of allowed Bragg reflections.

analysis described later. The technique of partial profile relaxation[20] was applied to 17 reflections in a region of *d* lager than 2.0 Å, which considerably improved fits between observed and calculated profiles for these reflections.

Tables 1 and 2 respectively list structural and geometrical parameters of the dehydrated sample with their estimated standard deviations in parentheses. Final *R* factors were $R_{wp} = 2.59\%$ ($R_e = 2.82\%$), $R_p = 1.95\%$, $R_B = 0.90\%$, and $R_F = 0.61\%$ with a Durbin-Watson statistic, d_{DW},[22] of 1.10. The lattice constant was $a = 24.53350(17)$ Å, and the unit-cell volume was $V = 14766.5(2)$ Å^3. Figure 1 shows observed, calculated, and difference patterns, where background intensities were subtracted from the observed and calculated ones.

Site Na1 lying perfectly on a six-membered ring was fully occupied. The number of Na2 atoms per eight-membered ring was ca. 0.97, with four equivalent positions per ring. All the fractional coordinates of atoms in the framework agreed closely with those reported by Adams et al.,[2,3] except for Na3. In our refinement, site Na3 was located at the center of a four-membered ring. The occupancy, *g*, of site Na3 is topologically ${}^1/_{12}$ (ref 23) but converged on 0.057(9). A Si/Al ratio of 1.010(9) suggests that the amount of substance for Si is nearly equal to that for Al. The chemical composition derived from the *g* values in Table 1 was $Na_{92.74}Si_{96.96}Al_{95.04}O_{384}\cdot 6.92H_2O$. The amount of substance for Na was a little smaller than that of Al. This result suggests that part of the Na^+ ions were exchanged by H_3O^+ ions while Na-LTA was washed. In this refinement, we could not detect adsorbed water unambiguously; the occupancies of O4, O5, O6, and O7 in cages were almost negligible. B_{eq}(Na2) as high as

(22) Young, R. A. In *The Rietveld Method*; Young, R. A., Ed.; Oxford University Press: Oxford, 1995; Chapter 1.

(23) Yanagida, R. Y.; Amaro, A. A.; Seff, K. *J. Phys. Chem.* **1973**, *77*, 805.

Table 3. Structure Parameters Determined for Dehydrated Na-LTA by X-ray Powder Diffraction

atom	site	*g*	*n*	*x*	*y*	*z*	*B*/Å^2
Si1	96i	1	96.00	0	0.0928(5)	0.1859(5)	2.59(8)
Si2	96i	0.01	0.960	0	0.1862(6)	0.0899(5)	=*B*(Si1)
Al	96i	0.99	95.04	0	=*y*(Si1)	=*z*(Si1)	=*B*(Si1)
O1	96i	1	96.00	0	0.1141(3)	0.2485(10)	2.8(2)
O2	96i	1	96.00	0	0.1462(8)	0.1465(9)	3.0(3)
O3	192j	1	192.00	0.0533(4)	0.0598(4)	0.1699(2)	2.8(2)
Na1	64g	1	64.00	0.10153(11)	=*x*	=*x*	4.3(2)
Na2	96i	0.2421	23.24	0	0.283(3)	0.280(3)	5.8(2)
Na3	96h	0.057	5.47	1/4	0.061(2)	=*y*	3.3(2)
WO1	192j	0.0282(12)	5.28	0.097(2)	0.048(10)	0.048(18)	3.8(3)
WO2	192j	=*g*(WO1)	5.28	=*y*(WO1)	=*x*(WO1)	=*z*(WO1)	=*B*(WO1)
WO3	192j	0.0877(9)	16.83	0.0316(9)	0.7984(13)	0.270(2)	3.6(4)
WO4	192j	=*g*(WO3)	16.83	=*y*(WO3)	=*x*(WO3)	=*z*(WO1)	=*B*(WO3)

4.8 Å^2 implies that other kinds of atoms are incorporated near this site. The average bond length was 1.61 Å for Si−O bonds and 1.73 Å for Al−O bonds. These bond lengths are in good agreement with those reported before.[1−3]

Structure Refinements with the XRD Data

The XRD data were analyzed with a Rietveld-refinement program RIETAN-98 for angle-dispersive diffraction.[21,24] RIETAN-98 has several new features such as split-type pseudo-Voigt and Pearson VII profile functions,[26] partial profile relaxation,[20,25] two peak-shift functions with forms of Legendre polynomials, output of files for MEM analysis, and analysis of the intensity data collected by varying step widths and/or counting times. These features were fully utilized in our Rietveld refinements. In the initial structural model for the dehydrated sample, the occupancies of cations were set at those refined in the neutron Rietveld analysis listed in Table 1. The positions of adsorbed water molecules in cages were estimated with EDD maps derived by the MEM; for convenience, details in the MEM analysis will be described in the next section. On the other hand, the initial coordinates of oxygen in adsorbed water were taken from crystal data in the literature.[6] These water molecules are situated around Na^+ ions attracting negative charges.

Partial profile relaxation[20,24] was applied to 11 reflections in a range of 2θ lower than 36° for the dehydrated sample and 15 reflections in a range of 2θ lower than 45° for the hydrated one. A modified split-type pseudo-Voigt function, where the full-widths-at-half-maximum (fwhm's) of Gaussian and Lorentzian components differ from each other,[24] was fitted to observed profiles of these reflections. On the other hand, we fitted the split-type pseudo-Voigt function of Toraya[25] to the profiles of all the other reflections. In the dehydrated sample, lowering of crystallinity by heating mainly spread the fwhm's of reflection profiles in a higher 2θ region.

In the Rietveld analysis of the XRD data, an oxygen ion is usually substituted for a water molecule. In this analysis, a virtual chemical species named WO, whose atomic scattering factor is the sum of those for one oxygen and two hydrogen atoms, was located in place of water because hydrated Na-LTA includes a considerable amount of hydrogen atoms; strictly speaking, the contribution of hydrogen atoms to diffraction intensities should not be neglected. Though the scattering amplitude of hydrogen is quite small, it contributes slightly to diffraction intensities in a range of $\sin\theta/\lambda < 0.4$. Thus, low-angle (small $\sin\theta/\lambda$) reflections contain significant structural information about hydrogen atoms, but contributions of hydrogen atoms to diffraction intensities are too low to refine their structure parameters directly. With the O^- ion (nine electrons) instead of water, the total amount of substance for the O^- was ca. 10% more than that obtained with WO.

The numbers of total electrons were approximately the same in both cases. On the use of WO in the Rietveld analysis of the hydrated sample, the total number of adsorbed water molecules per unit cell was ca. 252. This value agrees well with ca. 248, the value determined by thermogravimetry under vacuum, justifying the validity of the approximation with WO.

Tables 3 and 4 list structural and geometrical parameters of the dehydrated sample, respectively. Tables 5 and 6 give corresponding parameters of the hydrated sample. Lattice constants and unit-cell volumes were respectively $a = 24.5693(3)$ Å and $V = 14831.4(3)$ Å^3 for the dehydrated sample and $a = 24.6077(8)$ Å and $V = 14900.92(8)$ Å^3 for the hydrated one. Final refinement indices were $R_{wp} = 7.69\%$ ($R_e = 5.77\%$), $R_p = 5.18\%$, $R_B = 1.68\%$, $R_F = 1.30\%$, and $d_{DW} = 0.99$ for the dehydrated

Table 4. Interatomic Distances, *l*, and Bond Angles, ϕ, Obtained for Dehydrated Na-LTA by X-ray Powder Diffraction[a]

l/Å		ϕ/deg	
Si1−O1	1.63(2)	O1−Si1−O2	107.6(9)
Si1−O2	1.63(2)	O1−Si1−O3	113.4(5)
Si1−O3,O3^{i}	1.590(11)	O1−Si1−O3^{i}	113.4(5)
Al1,Si2−O1^{ii}	1.71(2)	O2−Si1−O3	105.3(6)
Al1,Si2−O2	1.70(2)	O2−Si1−O3^{i}	105.3(6)
Al1,Si2−O3^{iii},O3^{iv}	1.770(10)	O3−Si1−O3^{i}	110.9(6)
Na1−O2,O2^{iii},O2^{v}	2.940(2)	O1^{ii}−Al1,Si2−O2	104.9(3)
Na1−O3,O3^{iii},O3^{v}	2.298(4)	O1^{ii}−Al1,Si2−O3^{iii}	113.0(2)
Na2−O1^{vi}	2.627(9)	O1^{ii}−Al1,Si2−O3^{iv}	113.0(2)
Na2−O1^{vii}	2.726(9)	O2−Al1,Si2−O3^{iii}	106.5(2)
Na2−O2^{vi}	2.48(2)	O2−Al1,Si2−O3^{iv}	106.5(2)
Na2−O2^{vii}	3.727(9)	O3^{iii}−Al1,Si2−O3^{iv}	112.2(3)
Na3−O1^{v}	1.987(6)	Si1−O1−Al1^{vii}	140.8(6)
Na3−O3^{v}	1.976(6)	Si1−O2−Al1	161.7(6)
		Si1−O3−Al1^{v}	141.9(6)
Na2−WO2^{viii}	2.44(4)		
Na2−WO4^{ix}	2.45(4)		
WO1−WO2	1.7(3)		
WO1−WO2^{iii}	1.70(13)		

[a] Symmetry codes: (i) $-x, y, z$; (ii) $x, {}^1/_2 - z, y$; (iii) y, z, x; (iv) $-y, z, x$; (v) z, x, y; (vi) $-x, {}^1/_2 - y, {}^1/_2 - z$; (vii) $x, z, {}^1/_2 - y$; (viii) $-x, {}^1/_2 - z, 1 - y$; (ix) $-y, 1 - x, {}^1/_2 - z$.

(24) Izumi, F.; Ikeda, T. *Mater. Sci. Forum*, in press.
(25) Toraya, H. *J. Appl. Crystallogr.* **1990**, *23*, 485.
(26) Brown, I. D.; Altermatt, D. *Acta Crystallogr.* **1985**, *B41*, 244.

Table 5. Structure Parameters Determined for Hydrated Na-LTA by X-ray Powder Diffraction

atom	site	*g*	*n*	*x*	*y*	*z*	*B*/Å^2
Si1	96i	1	96.00	0	0.09242(13)	0.18481(12)	2.23(4)
Si2	96i	0.01	0.960	0	0.18401(12)	0.08963(11)	=*B*(Si1)
Al	96i	0.99	95.04	0	=*y*(Si1)	=*z*(Si1)	=*B*(Si1)
O1	96i	1	96.00	0	0.1126(2)	0.2463(3)	3.09(4)
O2	96i	1	96.00	0	0.1469(2)	0.1460(2)	3.58(5)
O3	192j	1	192.00	0.0516(3)	0.0576(2)	0.17214(13)	3.56(3)
Na1	64g	1	64.00	0.10290(8)	=*x*	=*x*	8.43(13)
Na2	96i	0.2421	23.24	0	0.244(2)	0.2827(6)	11.37(10)
Na3	96h	0.057	5.47	1/4	0.0417(9)	=*y*	6.49(12)
WO1	192j	0.1022(6)	19.63	0.0834(3)	0.018(3)	0.023(2)	8.1(4)
WO2	192j	=*g*(WO1)	19.63	=*y*(WO1)	=*x*(WO1)	=*z*(WO1)	=*B*(WO1)
WO3	64g	0.594(6)	38.04	0.1548(2)	=*x*	=*x*	7.5(3)
WO4	192j	0.278(2)	53.29	0.1154(2)	0.1634(2)	0.2685(3)	8.4(2)
WO5	192j	=*g*(WO5)	53.29	=*y*(WO4)	=*x*(WO4)	=*z*(WO4)	=*B*(WO4)
WO6	192j	0.149(2)	28.69	0.0637(4)	0.7693(6)	0.2905(6)	8.0(4)
WO7	192j	=*g*(WO6)	28.69	= *y*(WO6)	=*x*(WO6)	=*z*(WO6)	=*B*(WO6)
WO8	64g	0.158(6)	10.13	0.1896(9)	=*x*	=*x*	7.7(4)
WO9	8a	0.413(11)	3.30	1/4	1/4	1/4	4.6(5)

Table 6. Interatomic Distances, *l*, and Bond Angles, ϕ, Obtained for Hydrated Na-LTA by X-ray Diffraction[a]

l/Å		ϕ/deg	
Si1−O1	1.593(6)	O1−Si1−O2	107.5(3)
Si1−O2	1.649(7)	O1−Si1−O3	111.2(2)
Si1−O3,O3^{i}	1.561(3)	O1−Si1−O3^{i}	111.2(2)
Al1,Si2−O1^{ii}	1.799(6)	O2−Si1−O3	109.0(2)
Al1,Si2−O2	1.661(7)	O2−Si1−O3^{i}	109.0(2)
Al1,Si2−O3^{iii},O3^{iv}	1.728(4)	O3−Si1−O3^{i}	108.8(3)
Na1−O2,O2^{iii},O2^{v}	2.951(2)	O1^{ii}−Al1,Si2−O2	105.2(2)
Na1−O3,O3^{iii},O3^{v}	2.392(3)	O1^{ii}−Al1,Si2−O3^{iii}	109.42(9)
Na2−O1^{vi}	2.579(10)	O1^{ii}−Al1,Si2−O3^{iv}	109.42(9)
Na2−O1^{vii}	3.38(6)	O2−Al1,Si2−O3^{iii}	110.93(9)
Na2−O2^{vi}	2.99(4)	O2−Al1,Si2−O3^{iv}	110.93(9)
Na2−O2^{vii}	3.19(6)	O3^{iii}−Al1,Si2−O3^{iv}	110.72(14)
Na3−O1^{v}	2.042(9)	Si1−O1−Al1^{vii}	143.8(3)
Na3−O3^{v}	1.978(9)	Si1−O2−Al1	158.8(3)
		Si1−O3−Al1^{v}	148.6(3)
Na1−WO3	2.209(3)		
Na2−WO6^{viii}	1.621(12)		
Na2−WO7^{ix}	1.69(3)		
Na2−WO6^{xi}	2.459(11)		
Na2−WO7^{x}	2.41(2)		
WO3−WO8	1.48(3)		
WO8−WO9	2.57(2)		

[a] Symmetry codes: (i) $-x, y, z$; (ii) $x, {}^1/_2 - z, y$; (iii) y, z, x; (iv) $-y, z, x$; (v) z, x, y; (vi) $-x, {}^1/_2 - y, {}^1/_2 - z$; (vii) $x, z, {}^1/_2 - y$; (viii) $x, z, -{}^1/_2 + y$; (ix) $-y, z, 1 - x$; (x) $y, {}^1/_2 - z, -{}^1/_2 + x$; (xi) $-x, {}^1/_2 - z, 1 - y$.

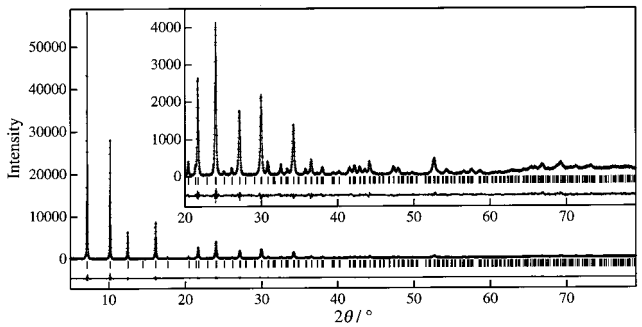

Figure 2. Rietveld-refinement patterns for the XRD data of the dehydrated sodium-type zeolite LTA. The inset shows magnified patterns from 20° to 80°.

sample and $R_{wp} = 6.94\%$ ($R_e = 5.30\%$), $R_p = 4.83\%$, $R_B = 2.45\%$, $R_F = 2.43\%$, and $d_{DW} = 1.02$ for the hydrated one. Figures 2 and 3 respectively give observed, calculated, and difference patterns of the dehydrated and hydrated samples, exhibiting excellent fits between the observed and calculated patterns.

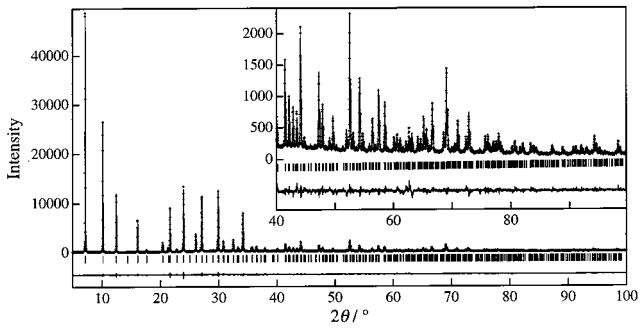

Figure 3. Rietveld-refinement patterns for the XRD data of the hydrated sodium-type zeolite LTA. The inset shows magnified patterns from 40° to 80°.

Bond lengths, *l*, in the framework had similar tendencies for the two samples. By calculating bond valence sums,[27] we predict *l*(Si−O) to be 1.62 Å and *l*(Al−O) to be 1.65 Å for tetrahedral coordination. The averages of Si−O distances calculated from the refined lattice and structure parameters are close to predicted distances: 1.59 Å in the hydrated sample and 1.61 Å in the dehydrated one. On the other hand, the averages of Al−O distances evaluated in the same fashion are somewhat larger than the expected ones, i.e., 1.73 Å in the hydrated sample and 1.74 Å in the dehydrated one. These distances in the dehydrated sample were almost the same as those obtained from the neutron diffraction data. Such elongation of Al−O bonds is quite usual in aluminosilicates containing cations in cages or channels. The framework in Na-LTA is negatively charged; electrical neutrality can be appropriately maintained by including Na^+ ions in cages, as described above.

Determination of EDD by MEM Analysis

Detailed spatial arrangements of adsorbed water molecules were determined by combined Rietveld and MEM analyses. Observed structure factors, F_o, and their estimated standard deviations, σ, were calculated from the observed and calculated profiles according to procedures described by Rietveld[28] and Kumazawa et al.,[29] respectively. The F_o's were analyzed by the MEM

(27) Brese, N. E.; O'Keeffe, M. *Acta Crystallogr.* **1991**, *B47*, 191.
(28) Rietveld, H. M. *J. Appl. Crystallogr.* **1969**, *2*, 65.
(29) Kumazawa, S. D. Eng. Thesis, Nagoya University, Nagoya, 1995.

with a FORTRAN program, MEED, developed by Kumazawa et al.[30] After EDD maps had been plotted with MEVIUS, structural models were modified, if necessary, by comparing them with the EDD images. In other words, we read approximate fractional coordinates of atoms incorporated in cages from the EDD images and refined their structure parameters by the Rietveld method. Rietveld refinements and MEM analyses were repeated alternately in such a manner until their results became consistent with each other.

In MEM analysis, we set space resolution to 128 × 128 × 128 pixels per unit cell and define R factors as

$$R_F = \sqrt{\frac{\sum|F_o - F_{MEM}|}{\sum|F_o|}}$$

and

$$wR_F = \sqrt{\frac{\sum\frac{1}{\sigma^2}|F_o - F_{MEM}|}{\sum\frac{1}{\sigma^2}|F_o|}}$$

where F_{MEM} is the structure factor estimated by MEM analysis and the summation is carried out over all reflections analyzed by the MEM.[29] The analysis of 344 F_o values for reflections in the region $d < 1.02$ Å yielded final R factors of $R_F = 1.68\%$ and $wR_F = 1.15\%$ in the hydrated sample. For 211 reflections in a region $d <$ 1.21 Å, R factors were $R_F = 1.41\%$ and $wR_F = 0.99\%$ in the dehydrated sample. These d ranges were selected by considering σ values and the dependence of crystallinity on the qualities of the samples.

Figure 4 gives the EDD maps of the (100) plane for the dehydrated and hydrated samples. In the dehydrated sample, site Na2 is clearly visible, and no localized electron densities were detected inside the β-cage. On the other hand, site Na2 is blurred and displaced from the above position in the hydrated sample. Localized peaks with low electron densities assigned to water were distributed near the four-membered ring in the β-cage. They correspond to sites WO1 and WO2 in the X-ray Rietveld refinements. The inclusion of residual water is in accord with the previous finding that water molecules in the β-cages cannot be removed perfectly.[31]

Figure 5 shows the EDD maps of the (400) planes for the dehydrated and hydrated samples, with the center of the α-cage on this plane. In the dehydrated sample, the α-cage contained no peaks due to localized electron densities, whereas sites WO3 and WO4 could be seen across the eight-membered ring. Part of the water molecules must be trapped at site Na2 by interaction with Na^+ ions on the removal of water through eight-membered rings during dehydration. Water molecules were distributed at both sides of site Na2 across the eight-membered ring in the hydrated sample. The low

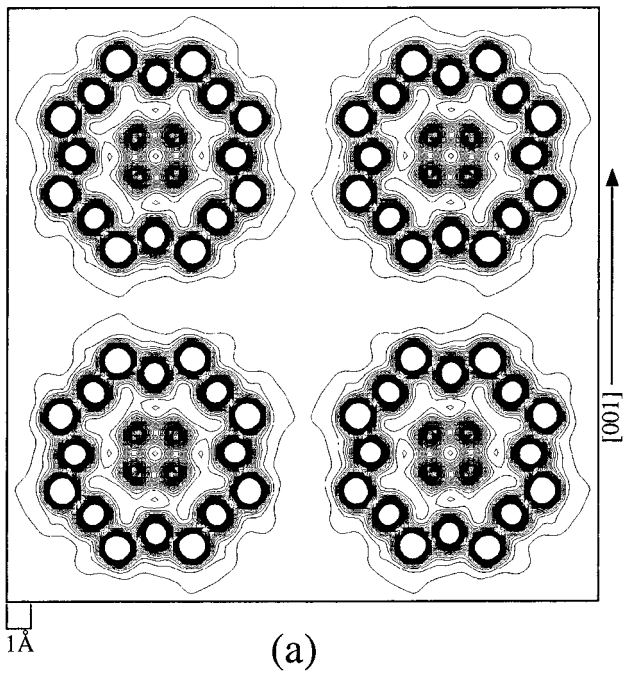

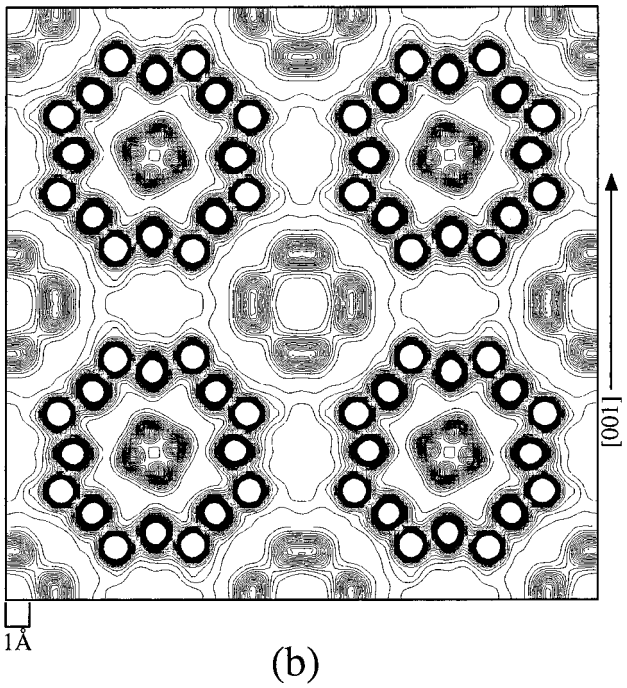

Figure 4. EDD on the (100) section in the (a) dehydrated and (b) hydrated samples. Contours were plotted with an interval of 0.1 e/Å^3 from 0.1 to 5.0 e/Å^3 in panel a and from 0.15 to 5.0 e/Å^3 in panel b.

electron densities for site Na2 spread out considerably. The apparently large atomic displacement parameter, B(Na2), supports the idea that Na2 is statically displaced from the average position by electrostatic interaction with water. Eight equivalent positions in the α-cage correspond to a couple of sites, WO4 and WO5, with the largest occupancies of all the WO sites. When overlapping these two to locate them at the same site with a z coordinate of ca. 0.25, their B parameters converged on extraordinary values larger than 10 Å^2. The EDD map yielded by the subsequent MEM analysis

(30) Kumazawa, S.; Kubota, Y.; Takata, M.; Ishibashi, Y. *J. Appl. Crystallogr.* **1993**, *26*, 453.
(31) Kodaira, T.; Takeo, H.; Nozue, Y. In *Proceedings, Science and Technology of Atomically Engineered Materials*; Jena, P., Khanna, S. N., Rao, B., Eds.; World Scientific: Singapore, 1995; p 85.

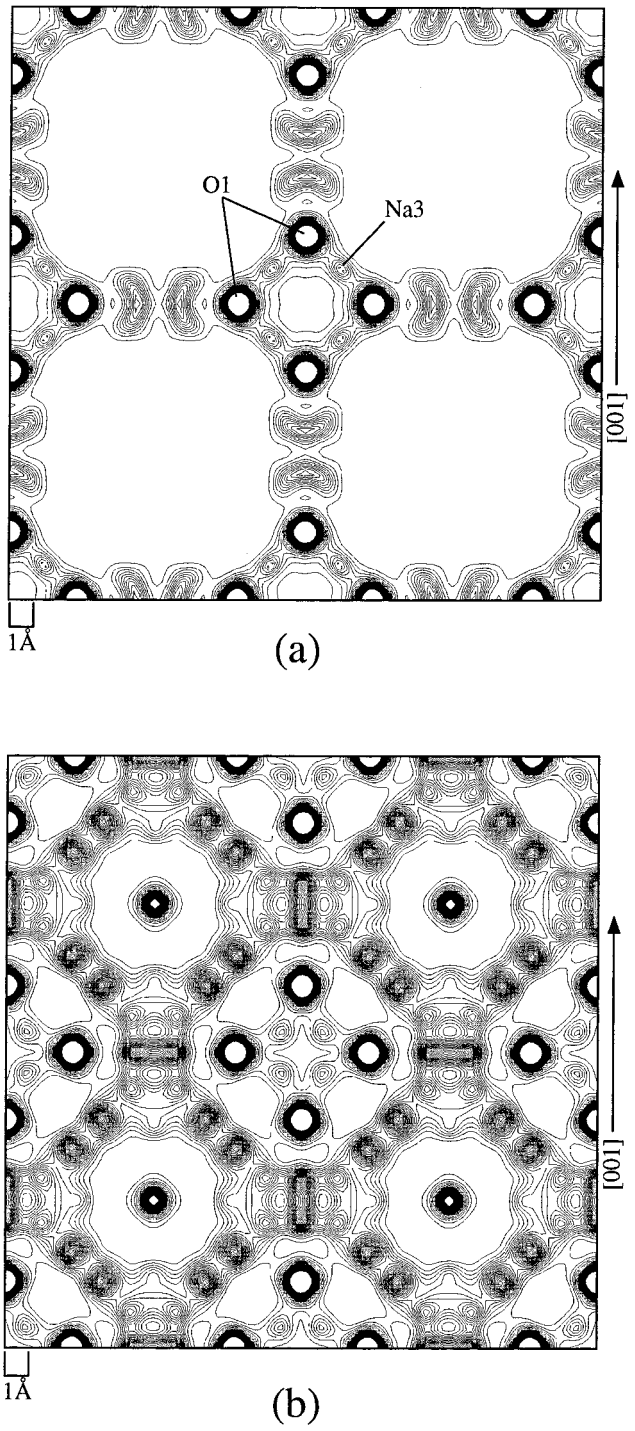

Figure 5. EDD on the (400) section in the (a) dehydrated and (b) hydrated samples with contours plotted in the same way as in Figure 4.

revealed that this atom splits into two pieces, whose electron densities spread toward site Na2. By contrast, neither of these two appeared in a Fourier-synthesis map. The refinement of the *z* coordinates for these two sites decreased R_{wp} from 9.54% to 7.03%.

Figure 6 shows the EDD maps of the (110) plane for the two samples. A β-cage surrounded by four α-cages is centered in these maps. In the dehydrated sample, localized and low-level peaks of electron densities are visible beside site Na1 inside the β-cage. These peaks, which are assigned to residual water WO1 and WO2, were also detected by the MEM, even without including

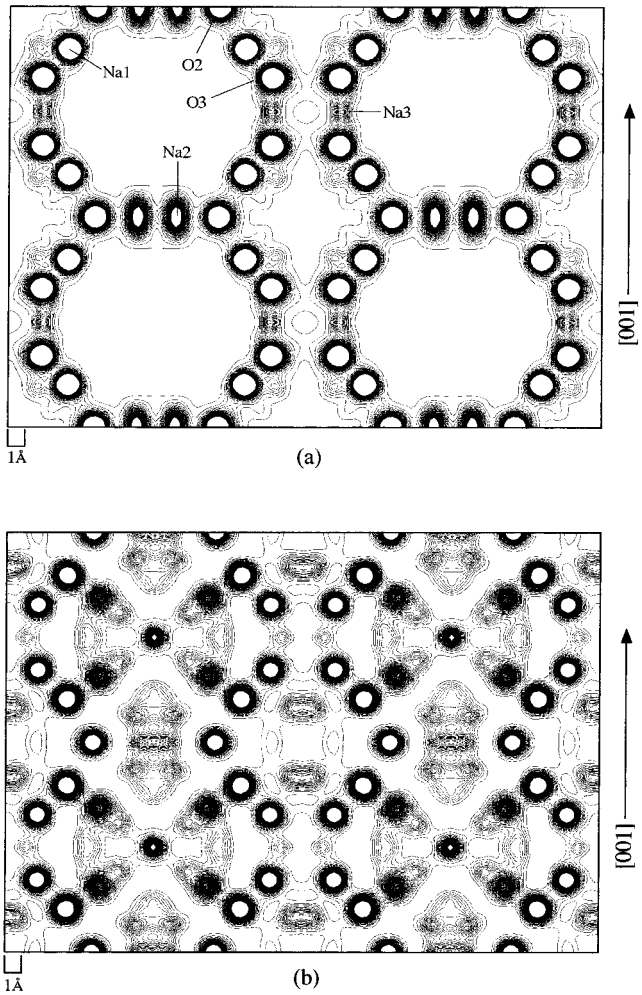

Figure 6. EDD on the (110) section in the (a) dehydrated and (b) hydrated samples with contours plotted in the same way as in Figure 4.

them in a structural model for Rietveld refinement. They may be also trapped by electrostatic attraction of Na1 ions. Site Na2 was not concentrated at one spot but dimmed by adjacent water in a similar way as in Figure 5. The α- and β-cages contain only very low electron densities inside it, with contours concentrated within the framework. Site Na3 was also found near the center of the four-membered ring constructing the α-cage. By contrast, these low-density sites could be hardly seen in a Fourier map (Figure 7). In Figure 7, sites WO1, WO2, and Na3 were invisible, whereas strong ghost peaks appeared near the center of the α-cage because of the termination effect. The Fourier map is of poor quality and full of illusory "ripples".

In the hydrated sample, high electron densities were observed beside sites Na1 and Na2. Localized low densities were also visible near the center of the α-cage, where no site was located in the initial structural model because the above positions were regarded as metastable ones with a high potential energy. The structural model was then modified to add them as sites WO8 and WO9. The occupancy of site WO9 converged on 0.41, which is close to a *g*(WO9) value of 0.39 evaluated from the EDD map by summing up electron densities for WO9. In the α-cage, a series of distinct peaks corresponding to a chain Na1−WO3−WO8−WO9−WO8−

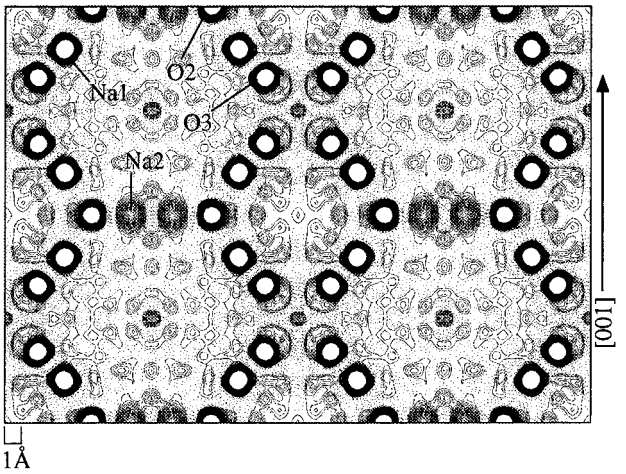

Figure 7. Fourier synthesis on the (110) section in the dehydrated samples with contours plotted an interval of 0.12 e/Å^3 from −1.0 to 5.0 e/Å^3.

WO3−Na1 extends along the [111] direction. This chain may be formed in such a manner as $Na^+\cdots(OH^{\delta-}\cdots H^{\delta+})\cdots(OH^{\delta-}\cdots H^{\delta+})\cdots Na^+$, where ··· denotes hydrogen and ionic bondings. Taking account of the geometrical symmetry for WO's and their bondings visible in the EDD map, water molecules corresponding to site WO9 are believed to be incorporated in α-cages, provided that the network-like chain is built up by clustering water molecules. Most WO sites corresponded to those in the structural model of Gramlich et al.[6] for a hydrated sample of Na-LTA.

Electron densities corresponding to site Na3 were observed in double four-membered rings (D4R), which is not consistent with a previous finding that site Na3 (≈0.25, 0.062, 0.062) is situated not in the D4R but in the α-cage.[2,3,32] The appearance of these low-density peaks is inconsistent with the conclusion of Papoular and Cox,[11] who insisted that site Na3 seen in their EDD map probably arose from the truncation effect and that its occupancy was nearly zero in their Rietveld refinement. The position of site Na3 determined in our refinement was far from that in their EDD map. Site Na3 was hardly visible in the D4R in an EDD map plotted by Fourier synthesis with F_o values obtained in the neutron Rietveld analysis unless it was included in its structural model. When fixing the coordinates of site Na3 at those obtained by Adams et al.,[2,3] the resulting Fourier-synthesis map displayed a peak with approximately the same coordinates inside the D4R. Though the difference between these two models could be hardly distinguished in difference-synthesis maps, g(Na3) converged on 0.057(8) in the neutron Rietveld analysis. The coordinates of site Na3 refined with both the TOF neutron and XRD data of the dehydrated sample differed considerably from those reported by Adams et al.[2,3] Our coordinates of Na3 were consistent with those estimated from the EDD images obtained by the MEM analysis. The Na3−O1 and Na3−O3 bond lengths of ca. 2.0 Å are, however, too short for an Na^+ ion in the four-membered ring because the effective window size of the four-membered ring is about 2.3 Å. This size is only slightly larger than the ionic radius of Na^+, 1.13 Å.[33] Two possible models can be proposed for the chemical species located at site Na3: (a) site Na3 may be occupied not by an Na^+ ion but by an H_3O^+ ion or (b) an Na^+ ion is stabilized to be confined in the D4R during framework formation. At present, we can hardly draw a definite conclusion concerning the chemical species in the D4R only from the present results. The amounts of Na^+ ions and adsorbed water molecules depend on conditions of sample preparation, and the ideal occupancy of site Na3 is only $^1/_{12}$. No other analytical methods can present unambiguous evidence for the occupation of site Na3. At any rate, we believe site Na3 to be occupied by some chemical species.

Concluding Remarks

The present structure refinements and MEM analyses of the hydrated and dehydrated Na-LTA's demonstrated that the distribution of adsorbed water molecules can be successfully visualized by combination of the Rietveld method and the MEM with the XRD data. From the EDD images, we can safely conclude that adsorbed water molecules were distributed beside Na^+ ions, changing the positions of the cations a little. TOF neutron powder diffraction was also effective for determining the accurate structure parameters of the atoms in the framework. The neutron and X-ray Rietveld refinements of the dehydrated sample gave essentially the same crystal structure and the distribution of Na^+ ions.

As far as known to us, no papers have hitherto been published on the structure analysis of zeolites by this combinational technique. It is particularly useful for modifying imperfect structural models and representing disordered structures, making it possible to reproduce true EDD from XRD data. With the improved goniometer and the advanced crystallographic programs RIETAN-98 and MEED, we could determine the detailed structures of the two samples for Na-LTA.

In the present combined methods, F_o's were calculated by partitioning observed intensities among overlapping reflections in proportion to their profiles calculated from final structural parameters in Rietveld analysis.[29] Consequently, EDDs derived by the MEM in the combined methods are more or less biased by the structural model in Rietveld analysis. The MEM can, however, provide us with valuable information about structural details, including covalent bonds, positional disordering, defects, and sites occupied partially. Because zeolites have relatively complex structures with large unit-cell volumes, only the application of the Rietveld method is the practical way to get F_o's for MEM analysis with powder samples.

There is still room for improving the accuracies of structure parameters for Na-LTA. The performance of the combined Rietveld and maximum-entropy methods would be enhanced if synchrotron XRD patterns with much higher resolution could be measured. With synchrotron XRD data, the F_o's of reflections in the small d region can be determined more accurately and more precisely with an increase in effective space resolution. The resulting EDD maps display nearly

(32) Pluth, J. J.; Smith, V. *J. Am. Chem. Soc.* **1979**, *83*, 741.

(33) Shannon, R. D. *Acta Crystallogr.* **1976**, *A32*, 751.

"true electron densities" and clearer structural details with a larger number of pixels. If the crystallinity of dehydrated Na-LTA were made better by changing heating conditions, their structural details could be viewed more clearly. Nevertheless, the amount of adsorbed water determined by our X-ray Rietveld refinement of the dehydrated sample well agrees with that measured by thermogravimetry, and the EDD images resulting from the combined methods successfully express the atomic distribution in the cages. In the case of the dehydrated sample, sites WO1−WO4 were scarcely occupied: 0.028 for WO1 and WO2 and 0.088 for WO3 and WO4. Hence, the combined technique has enabled us to estimate the positions of the guests despite their very low occupancies.

Acknowledgment. We thank K. Oikawa of the Japan Atomic Energy Research Institute for his assistance in measuring the TOF neutron powder diffraction data and Y. Kiyozumi of the National Institute of Materials and Chemical Research for helpful advice on the preparation of the samples.

CM980442Y